Coastal Southern Ocean: A strong anthropogenic CO_2 sink

Kevin R. Arrigo,[1] Gert van Dijken,[1] and Matthew Long[1]

Received 7 August 2008; revised 22 September 2008; accepted 1 October 2008; published 7 November 2008.

[1] Large-scale estimates of the Southern Ocean CO_2 sink do not adequately resolve the fluxes associated with Antarctic continental shelves. Using a mechanistic three-dimensional biogeochemical model of the Ross Sea, we show that Antarctic shelf waters are a strong sink for CO_2 due to high biological productivity, intense winds, high ventilation rates, and extensive winter sea ice cover. Net primary production (NPP) in these waters is $\sim$0.055 Pg C yr^{-1}. Some of this carbon sinks to depth, driving an influx of CO_2 of 20–50 g C m^{-2} yr^{-1}. Although currently unaccounted for, the total atmospheric CO_2 sink on the Ross Sea continental shelf of 0.013 Pg C yr^{-1} is equivalent to 27% of the most recent estimate of the CO_2 sink for the entire Southern Ocean. Given these results, these and other highly productive waters around the Antarctic continent need to be included in future budgets of anthropogenic CO_2.
Citation: Arrigo, K. R., G. van Dijken, and M. Long (2008), Coastal Southern Ocean: A strong anthropogenic CO_2 sink, *Geophys. Res. Lett.*, *35*, L21602, doi:10.1029/2008GL035624.

1. Introduction

[2] Of the 7–9 Pg C yr^{-1} released as CO_2 into the atmosphere by humans, 25–35% is taken up by the ocean through physical and biological processes. A variety of methods have been employed to assess the role of the ocean as a sink for atmospheric CO_2, including atmospheric and oceanic inversions, analysis of transient tracers, measured (or inferred) surface ocean partial pressure of CO_2 (pCO_2), and global climate models. These techniques generally agree that the largest CO_2 sinks are found in the North Atlantic and the Southern Ocean, but disagree as to the magnitude of these sinks, particularly in the Southern Ocean, where historical estimates range widely from 0.10 to 0.56 Pg C yr^{-1} [*Takahashi et al.*, 2002; *Gloor et al.*, 2003; *Roy et al.*, 2003; *Gurney et al.*, 2004; *Sabine et al.*, 2004; *Wetzel et al.*, 2005; *Mikaloff Fletcher et al.*, 2007; *McNeil et al.*, 2007]. However, the most recent analysis of the largest available observational pCO_2 data set supports estimates at the lower end of this range, suggesting that the Southern Ocean removes only 0.05 Pg C yr^{-1} from the atmosphere (T. Takahashi et al., Climatological mean and decadal change in surface ocean pCO_2 and net sea-air CO_2 flux over the global oceans, submitted to *Global Biogeochemical Cycles,* 2008). Unfortunately, all of these estimates are of low spatial resolution, making it impossible for them to fully resolve many of the most productive regions of the Southern Ocean, including much of the continental shelf (waters of <1000 m depth) and its associated coastal polynyas (areas of open water surrounded by sea ice), where the air-sea flux of CO_2 (FCO_2) is expected to be relatively high.

[3] The narrow continental shelves around Antarctica are important ventilation sites because they are regions of active Antarctic Bottom Water (AABW) formation [*Jacobs et al.*, 1970, 1985; *Gordon et al.*, 2004]. Beginning in austral autumn, cold and intense offshore winds initiate the growth of sea ice within the coastal polynyas (Figure 1a) that ring the Antarctic continent [*Arrigo and Van Dijken*, 2003]. As the associated rejection of salt increases surface salinity, these dense waters sink, driving deep convection and bringing waters high in both nutrients and CO_2 to the surface. Once the sea ice melts in spring, some CO_2 escapes to the atmosphere, but because surface nutrient and trace metal concentrations on the shelf are high [*Fitzwater et al.*, 2000; *Coale et al.*, 2005], intense phytoplankton blooms develop, rapidly reducing pCO_2 to very low levels [*Sweeney*, 2003]. Some of this newly fixed organic carbon sinks below the surface layer, driving an influx of atmospheric CO_2. How much total carbon is exported off the shelf, including the anthropogenic component (C_{ant}), is currently not known.

2. Methods

[4] To quantify the importance of the Antarctic continental shelf and its associated coastal polynyas as sinks for anthropogenic CO_2, we implemented a coupled physical/biogeochemical model of the southwestern Ross Sea [*Arrigo et al.*, 2003] with the spatial resolution required to accurately simulate phytoplankton dynamics and CO_2 fixation, carbon export, and air-sea CO_2 exchange on the shelf in response to physical forcing (for model validation see auxiliary material[1]). The Coupled Ice, Atmosphere, and Ocean (CIAO) model was run over an annual cycle with identical biology under both pre-industrial (280 μatm) and contemporary (380 μatm) atmospheric pCO_2 conditions; anthropogenic CO_2 fluxes and inventories were calculated as the difference between these two runs. Model physics were spun up under climatological forcing for 80 years, at which time the biogeochemical components of the model were switched on and the model was run until the carbon system on the continental shelf had reached steady-state (10 years, about double the residence time of water on the shelf [*Jacobs et al.*, 1970]).

3. Results and Discussion

[5] The spatial pattern of modeled annual net primary production (NPP) by phytoplankton on the Ross Sea con-

[1]Department of Environmental Earth System Science, Stanford University, Stanford, California, USA.

0094-8276/08/2008GL035624$05.00

[1]Auxiliary materials are available in the HTML. doi:10.1029/2008GL035624.

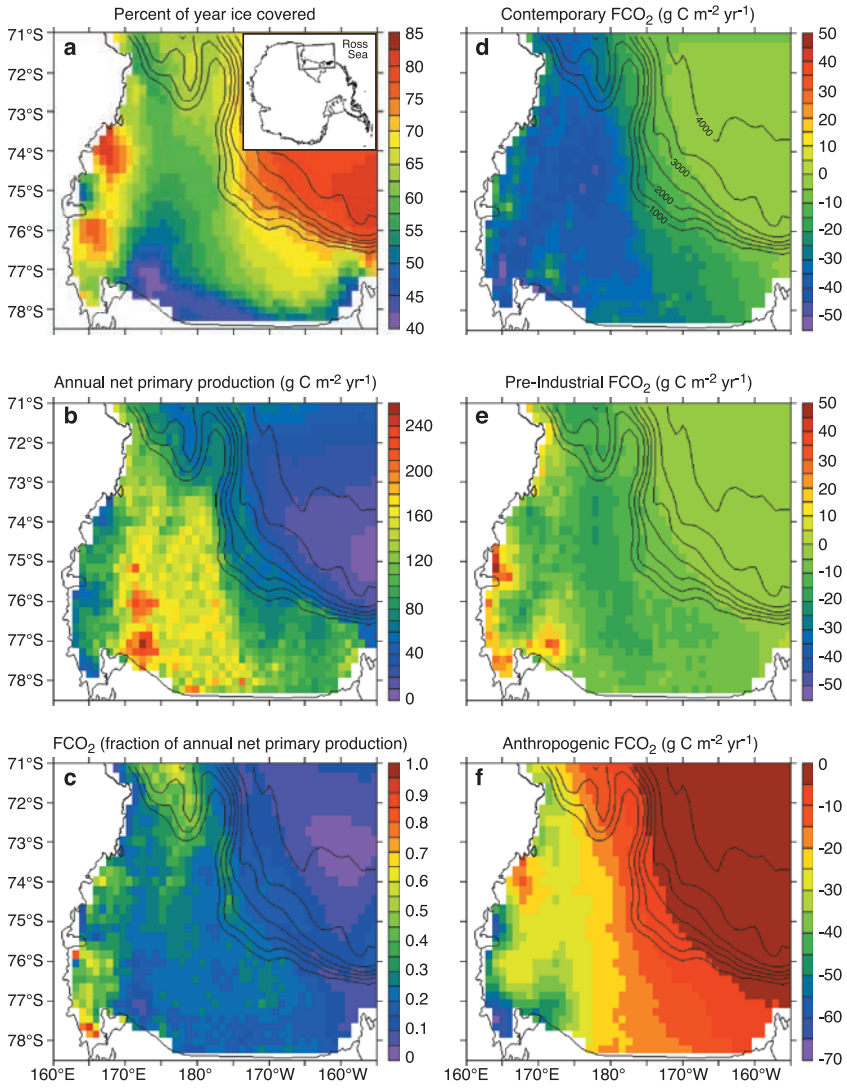

Figure 1

Figure 1. Sea ice cover, annual primary production, and air-sea flux of CO_2 (FCO_2) for the Ross Sea continental shelf. (a) Percent of the year that a given region was ice covered. (b) Annual net primary production (NPP). This was the same for all model runs. (c) Annual FCO_2 for the contemporary model run expressed as a percent of annual NPP. Negative sign denotes CO_2 flux from the atmosphere to the ocean. (d) Annual FCO_2 for the contemporary model run (atmospheric CO_2 = 380 μatm). (e) Annual FCO_2 for the pre-industrial model run (atmospheric CO_2 = 280 μatm). (f) Annual anthropogenic FCO_2, calculated as the difference between Figures 1d and 1e.

tinental shelf (Figure 1b), which is the same in the pre-industrial and contemporary model runs, agrees well with estimates made both in situ [*Arrigo et al.*, 2000] and using satellite ocean color data [*Arrigo and Van Dijken*, 2004, 2007; *Arrigo et al.*, 2008]. Annual NPP is highest (and pCO_2 lowest) in the relatively ice-free central Ross Sea polynya region (Figure 1a), ranging from ~140 to >200 g C m^{-2} yr^{-1} (Figure 1b). NPP is lower along the western side of the continental shelf (west of 170°E) where ice cover is more persistent (Figure 1a) and strong winds mix the water column more deeply. The off-shelf waters in the northeast sector of our study region exhibit extremely low annual NPP because of persistent sea ice cover and low trace metal concentrations [*Fitzwater et al.*, 2000; *Coale et al.*, 2005]. Total NPP on the Ross Sea continental shelf is approximately 54.7 Tg C yr^{-1}.

[6] In winter, surface waters of the Ross Sea are supersaturated in pCO_2 (~425 μatm, Figure 2a) due to upwelling of deep, high CO_2 water onto the shelf and convective mixing, initiated by cooling and brine rejection during sea ice formation, that mixes this high CO_2 water to the surface. Once sea ice melts in the austral spring and light becomes sufficient to support net phytoplankton growth, rates of NPP increase and surface pCO_2 in the polynya is rapidly reduced to below atmospheric levels in both the pre-industrial and contemporary runs (Figure 2a). Surface pCO_2 on the shelf drops to as low as 150 μatm at the peak of the phytoplankton bloom and persists at low levels from December through

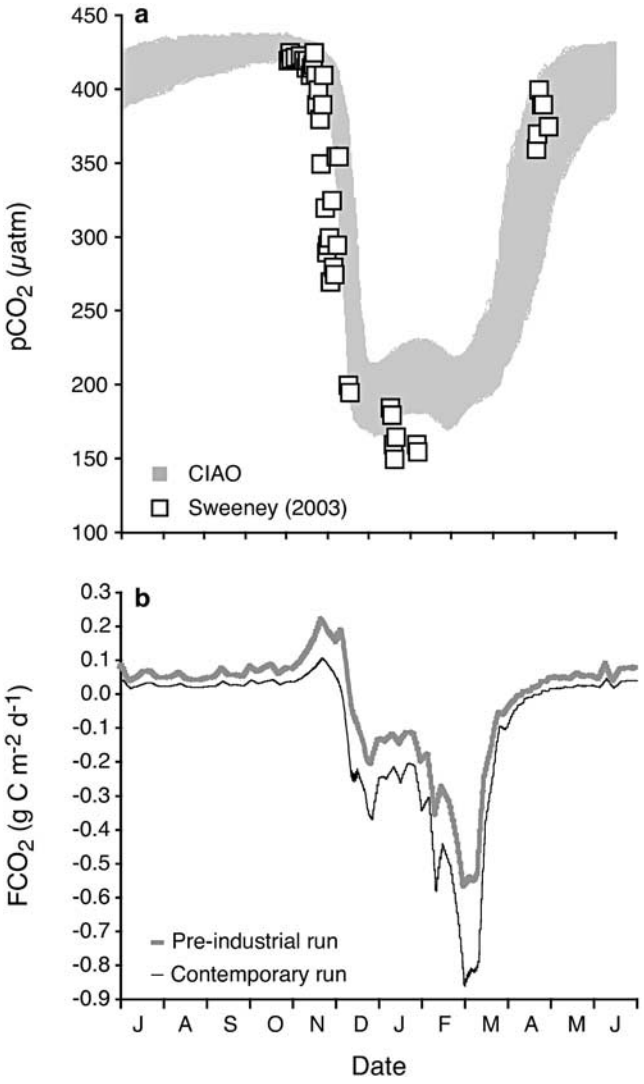

Figure 2. Surface partial pressure of CO_2 (pCO_2) and associated FCO_2 for the Ross Sea. (a) Time series of surface pCO_2 on the Ross Sea continental shelf predicted by the CIAO model (contemporary run) and measured by *Sweeney* [2003]. (b) Changes in FCO_2 on the Ross Sea continental shelf over an annual cycle predicted by CIAO for the pre-industrial and contemporary model runs. Negative values denote fluxes from the atmosphere into the ocean and are greatest when surface pCO_2 is low and wind speeds are high.

March in both model runs, in excellent agreement with in situ observations (Figure 2a). The calculated summer surface pCO_2 deficits are virtually identical for the two runs because both NPP and the CO_2 content of the waters that upwell onto the continental shelf (and eventually into surface waters) are assumed to be the same. Although intermediate waters of the Southern Ocean have 10–30 μmol kg^{-1} more total CO_2 (TCO_2) today than they had in pre-industrial times [*Sabine et al.*, 2004], the assumption in the model that subsurface TCO_2 has remained unchanged impacts estimates of FCO_2 by only <3% (see sensitivity analysis in auxiliary material). Increased winds in late austral summer and autumn enhance FCO_2, with maximum fluxes of −0.55 and −0.85 g C m^{-2} d^{-1} (Figure 2b) in the pre-industrial and contemporary runs, respectively (negative sign denotes flux from atmosphere to ocean), causing surface pCO_2 to begin to rise in February (Figure 2a). Despite similar surface pCO_2 in the two runs, FCO_2 is higher in the contemporary run because its higher atmospheric pCO_2 results in a larger ΔpCO_2. Remineralization of organic matter and enhanced convective mixing of deep CO_2-rich waters into the surface layer also increase surface pCO_2, thereby reducing FCO_2 throughout March (Figure 2b). By April, newly-formed sea ice inhibits further CO_2 exchange even as surface water pCO_2 rises to >400 μatm (Figure 2a), in excess of atmospheric levels.

[7] In the contemporary run, annual FCO_2 ranges from −20 to −50 g C m^{-2} yr^{-1} in waters associated with the Ross Sea polynya (Figure 1d). The spatial distribution of the annual FCO_2 in both model runs is directly related to spatial variability in annual NPP (Figure 1b); high NPP leads to larger drawdown of CO_2, generating regions of low surface pCO_2 and a large ΔpCO_2. FCO_2 was also mostly negative in the pre-industrial run (Figure 1e), but because ΔpCO_2 was smaller than in the contemporary run (due to lower atmospheric pCO_2), so was FCO_2. FCO_2 depends not only on ΔpCO_2 but also on wind speed, and thus FCO_2, calculated as a fraction of NPP (Figure 1c), is greatest near the coast along the western margin of the continental shelf where winds are most intense. In these coastal regions, annual FCO_2 is equivalent to 40–70% of annual NPP.

[8] Because of its unique physical and biological characteristics, including high rates of ventilation and primary production, annual FCO_2 on the Ross Sea continental shelf, including less productive offshore waters with lower wind speeds, is remarkably high, amounting to −13.3 Tg C yr^{-1} (24% of annual NPP for these waters). Furthermore, approximately 70% of contemporary FCO_2 is anthropogenic, with C_{ant} fluxes ranging from −40 to −70 g C m^{-2} yr^{-1} along the western continental shelf (Figure 1f) and approximately −20 to −30 g C m^{-2} yr^{-1} further offshore. Surprisingly, although the Ross Sea continental shelf comprises only 0.36% of the open water area in the Southern Ocean south of 50°S, its annual rate of FCO_2 is equivalent to 27% of the most recent estimate of the total CO_2 sink for the entire Southern Ocean (which does not include the high FCO_2 we report for the Ross Sea continental shelf) (Takahashi et al., submitted manuscript, 2008). Total FCO_2 for all Antarctic continental shelves is likely to be considerably higher, since the Ross Sea accounts for only 20% of total shelf area around Antarctica (see auxiliary material). Our results suggest that Antarctic continental shelves, which are largely unaccounted for in global estimates of the air-sea flux of C_{ant}, may represent the most efficient long-term sinks of C_{ant} in the global ocean.

[9] Our physical model indicates that much of the CO_2 entrained in surface waters is ultimately moved off the shelf in the deep waters that form there. Because of active mixing and deep convection on the continental shelf, both the pre-industrial (Figure 3b) and anthropogenic (Figure 3c) components of contemporary TCO_2 (Figure 3a) penetrate to the bottom. In these shelf waters, concentrations of C_{ant} are approximately 12–25 μmol kg^{-1} throughout the water column, in good agreement with previous estimates of C_{ant} from the Ross Sea made using the MIX (C_{ant} = 10–

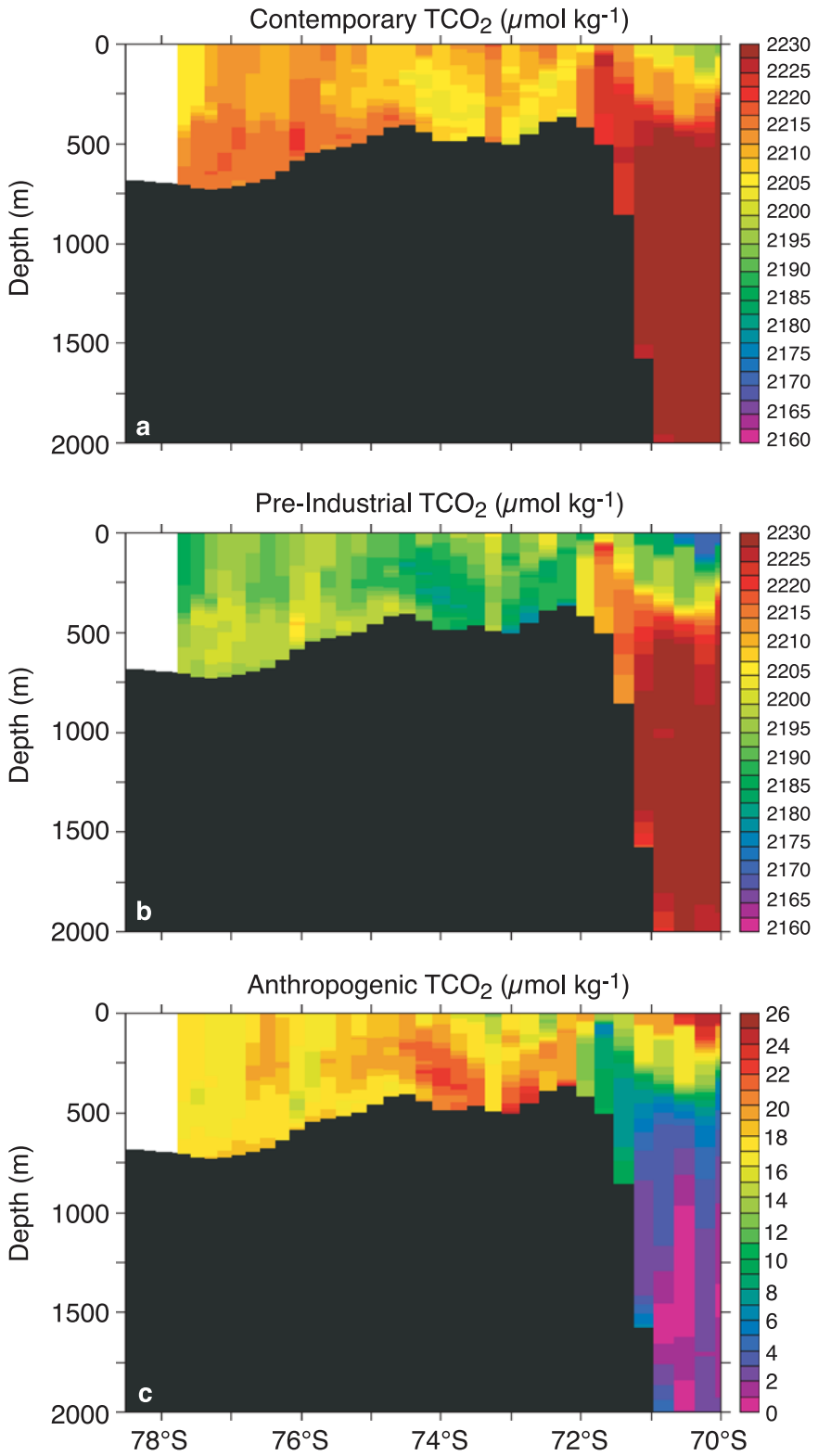

Figure 3. Total CO_2 (TCO_2) across the continental shelf of the Ross Sea. A latitudinal section along 171°E shows invasion of atmospheric CO_2 into the ocean interior on the Ross Sea continental shelf. (a) TCO_2 for the contemporary model run. (b) TCO_2 for the pre-industrial model run. (c) Anthropogenic TCO_2.

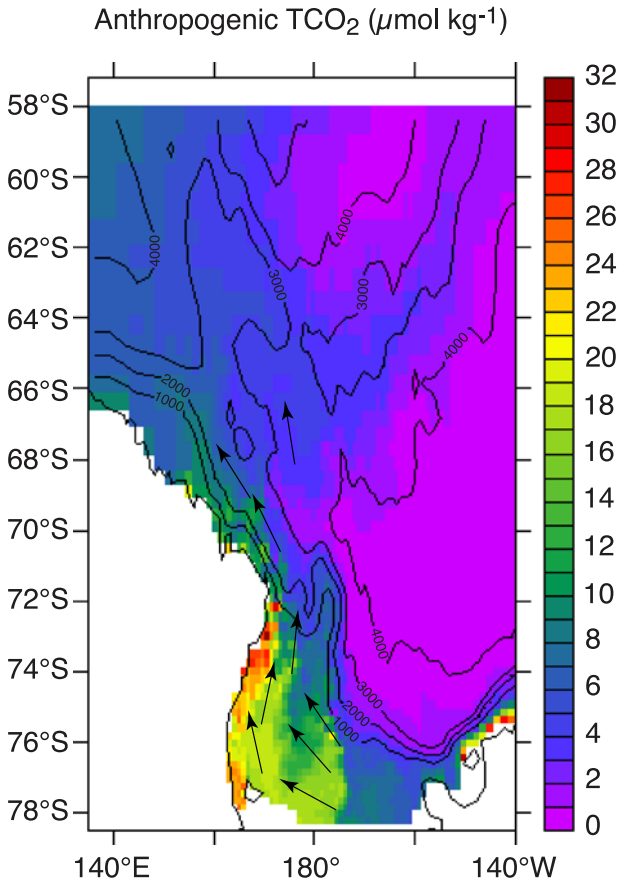

Figure 4. Anthropogenic TCO_2 in deep waters of the Ross Sea. As high-density waters sink and flow northeastward off the Ross Sea continental shelf, they carry anthropogenic CO_2 (C_{ant}) with them. Arrows show approximate direction of deep water flow.

25 μmol kg^{-1}) and TrOCA (C_{ant} = 12–30 μmol kg^{-1}) methods [*Sandrini et al.*, 2007]. Eventually, this deep C_{ant} is entrained in bottom waters that move downslope in a narrow northward-flowing plume along the western margin of the continental shelf (Figure 4). CIAO estimates that these waters flow off the shelf at a rate of 4.2–5.3 Sv (10^6 m^3 s^{-1}), consistent with previous measurements of off-shelf bottom water transport that range from 3.9–5.0 Sv [*Gordon*, 1974; *Häkkinen*, 1995; *Orsi et al.*, 1999]. Energetic plumes of dense water of the same temperature (−1.7°C to −0.8°C) and salinity (34.66 to 34.80) as those in the model were observed in this location during the AnSlope program [*Gordon et al.*, 2004], reaching velocities of 1 m s^{-1}. The saltiest waters observed on the Ross Sea continental shelf [*Jacobs et al.*, 1985; *Orsi et al.*, 1999] form in the western shelf region where FCO_2 is highest, providing an efficient mechanism for transporting C_{ant} into the deep ocean. After flowing down and off the shelf, these dense waters move northward and spread into the deep ocean, carrying C_{ant} with them (Figure 4).

[10] New approaches have hinted at the importance of Antarctic continental shelf processes in the sequestration of anthropogenic CO_2 [*Lo Monaco et al.*, 2005] but our study is the first to quantify the magnitude and distribution of this flux and to relate it to meteorological and oceanographic processes that are unique to the shelf environment. Recent evidence has suggested that the ability of much of the Southern Ocean to take up anthropogenic CO_2 may have decreased in the last two decades due to a poleward shift and intensification of westerly winds enhancing ventilation of deep CO_2-rich water [*Le Quere et al.*, 2007]. Additionally, it has been suggested that as more anthropogenic CO_2 enters the surface ocean, particularly in regions with strong stratification, the ability of the ocean to act as a CO_2 sink diminishes [*Le Quere et al.*, 2007]. While these processes may impact continental shelf systems, their effect will be minimized in regions with both high rates of primary production and vigorous deep-water ventilation, such as on the Antarctic continental shelf, where CO_2 can be efficiently transported from the surface to the deep ocean. Thus, the relative importance of anthropogenic CO_2 sinks in regions like the Antarctic continental shelf is likely to increase in years to come.

[11] **Acknowledgments.** This research was supported by the Ocean Carbon Sequestration Research Program, Biological and Environmental Research (BER), U.S. Department of Energy (grant DE-FG03-01ER63176) and the NASA Oceanography Program (grant NAG5-11264).

References

Arrigo, K. R., and G. L. van Dijken (2003), Phytoplankton dynamics within 37 Antarctic coastal polynyas, *J. Geophys. Res.*, *108*(C8), 3271, doi:10.1029/2002JC001739.

Arrigo, K. R., and G. L. van Dijken (2004), Annual changes in sea ice, *chlorophyll a*, and primary production in the Ross Sea, Antarctica, *Deep Sea Res., Part II*, *51*, 117–138.

Arrigo, K. R., and G. L. van Dijken (2007), Interannual variation in air-sea CO_2 flux in the Ross Sea, Antarctica: A model analysis, *J. Geophys. Res.*, *112*, C03020, doi:10.1029/2006JC003492.

Arrigo, K. R., G. R. DiTullio, R. B. Dunbar, M. P. Lizotte, D. H. Robinson, M. VanWoert, and D. L. Worthen (2000), Phytoplankton taxonomic variability and nutrient utilization and primary production in the Ross Sea, *J. Geophys. Res.*, *105*, 8827–8846.

Arrigo, K. R., D. L. Worthen, and D. H. Robinson (2003), A coupled ocean-ecosystem model of the Ross Sea: 2. Iron regulation of phytoplankton taxonomic variability and primary production, *J. Geophys. Res.*, *108*(C7), 3231, doi:10.1029/2001JC000856.

Arrigo, K. R., G. L. van Dijken, and S. Bushinsky (2008), Primary production in the Southern Ocean, 1997–2006, *J. Geophys. Res.*, *113*, C08004, doi:10.1029/2007JC004551.

Coale, K. H., R. M. Gordon, and X. J. Wang (2005), The distribution and behavior of dissolved and particulate iron and zinc in the Ross Sea and Antarctic circumpolar current along 170°W, *Deep Sea Res., Part I*, *52*, 295–318.

Fitzwater, S. E., K. S. Johnson, R. M. Gordon, K. H. Coale, and W. O. Smith (2000), Trace metal concentrations in the Ross Sea and their relationship with nutrients and phytoplankton growth, *Deep Sea Res., Part II*, *47*, 3159–3179.

Gloor, M., N. Gruber, J. Sarmiento, C. L. Sabine, R. A. Feely, and C. Rodenbeck (2003), A first estimate of present and preindustrial air-sea CO_2 flux patterns based on ocean interior carbon measurements and models, *Geophys. Res. Lett.*, *30*(1), 1010, doi:10.1029/2002GL015594.

Gordon, A. L. (1974), Varieties and variability of Antarctic bottom water, *Colloq. Int. C. N. R. S.*, *215*, 33–47.

Gordon, A. L., E. Zambianchi, A. Orsi, M. Visbeck, C. F. Giulivi, T. Whitworth III, and G. Spezie (2004), Energetic plumes over the western Ross Sea continental slope, *Geophys. Res. Lett.*, *31*, L21302, doi:10.1029/2004GL020785.

Gurney, K. R., et al. (2004), Transcom 3 inversion intercomparison: Model mean results for the estimation of seasonal carbon sources and sinks, *Global Biogeochem. Cycles*, *18*, GB1010, doi:10.1029/2003GB002111.

Häkkinen, S. (1995), Seasonal simulation of the Southern Ocean coupled ice-ocean system, *J. Geophys. Res.*, *100*, 22,733–22,748.

Jacobs, S. S., A. F. Amos, and P. M. Bruchhau (1970), Ross Sea oceanography and Antarctic Bottom Water formation, *Deep Sea Res.*, *17*, 935–962.

Jacobs, S. S., R. G. Fairbanks, Y. Horibe (1985), Origin and evolution of water masses near the Antarctic continental margin: Evidence from $H_2{}^{18}O/H_2{}^{16}O$ ratios in seawater, in *Oceanology of the Antarctic Conti-*

nental Shelf, Ant. Res. Ser., vol. 43, edited by S. S. Jacobs, pp. 59–85, AGU, Washington, D. C.

Le Quere, C., et al. (2007), Saturation of the Southern Ocean CO_2 sink due to recent climate change, *Science*, *316*, 1735–1738, doi:1126/science.1136188.

Lo Monaco, C., N. Metzl, A. Poisson, C. Brunet, and B. Schauer (2005), Anthropogenic CO_2 in the Southern Ocean: Distribution and inventory at the Indian-Atlantic boundary (World Ocean Circulation Experiment line I6), *J. Geophys. Res.*, *110*, C06010, doi:10.1029/2004JC002643.

McNeil, B. I., N. Metzl, R. M. Key, R. J. Matear, and A. Corbiere (2007), An empirical estimate of the Southern Ocean air-sea CO_2 flux, *Global Biogeochem. Cycles*, *21*, GB3011, doi:10.1029/2007GB002991.

Mikaloff Fletcher, S. E., et al. (2007), Inverse estimates of the oceanic sources and sinks of natural CO_2 and the implied oceanic carbon transport, *Global Biogeochem. Cycles*, *21*, GB1010, doi:10.1029/2006GB002751.

Orsi, A. H., G. C. Johnson, and J. L. Bullister (1999), Circulation, mixing, and production of Antarctic Bottom Water, *Prog. Oceanogr.*, *43*, 55–109.

Roy, T., P. Rayner, R. Matear, and R. Francey (2003), Southern Hemisphere ocean CO_2 uptake: Reconciling atmospheric and oceanic estimates, *Tellus, Ser. B*, *55*, 701–710.

Sabine, C. L., et al. (2004), The oceanic sink for anthropogenic CO_2, *Science*, *305*, 367–371.

Sandrini, S., N. Ait-Ameur, P. Rivaro, S. Massolo, F. Touratier, L. Tositti, and C. Goyet (2007), Anthropogenic carbon distribution in the Ross Sea Antarctica, *Ant. Sci.*, *19*, 395–407.

Sweeney, C. (2003), The annual cycle of surface water CO_2 and O_2 in the Ross Sea: A model for gas exchange on the continental shelves of Antarctica, in *Biogeochemistry of the Ross Sea, Antarct. Res. Ser.*, vol. 78, edited by R. B. Dunbar and G. R. DiTullio, pp. 295–312, AGU, Washington, D. C.

Takahashi, T., et al. (2002), Global sea-air CO_2 flux based on climatological surface ocean pCO_2, and seasonal biological and temperature effects, *Deep Sea Res., Part II*, *49*, 601–1622.

Wetzel, P., A. Winguth, and E. Maier-Reimer (2005), Sea-to-air CO_2 flux from 1948 to 2003: A model study, *Global Biogeochem. Cycles*, *19*, GB2005, doi:10.1029/2004GB002339.

K. R. Arrigo, M. Long, and G. van Dijken, Department of Environmental Earth System Science, Stanford University, Stanford, CA 94305-2215, USA. (arrigo@stanford.edu)